

# Teaching Agents how to Map: Spatial Reasoning for Multi-Object Navigation

Pierre Marza<sup>1</sup>, Laetitia Matignon<sup>2</sup>, Olivier Simonin<sup>3</sup> and Christian Wolf<sup>1</sup>

**Abstract**—In the context of visual navigation, the capacity to map a novel environment is necessary for an agent to exploit its observation history in the considered place and efficiently reach known goals. This ability can be associated with spatial reasoning, where an agent is able to perceive spatial relationships and regularities, and discover object characteristics. In classical Reinforcement Learning (RL) setups, this capacity is learned from reward alone. We introduce supplementary supervision in the form of auxiliary tasks designed to favor the emergence of spatial perception capabilities in agents trained for a goal-reaching downstream objective. We show that learning to estimate metrics quantifying the spatial relationships between an agent at a given location and a goal to reach has a high positive impact in Multi-Object Navigation settings. Our method significantly improves the performance of different baseline agents, that either build an explicit or implicit representation of the environment, even matching the performance of incomparable oracle agents taking ground-truth maps as input.

## I. INTRODUCTION

Navigating in a previously unseen environment requires different abilities, among which is mapping, i.e. the capacity to build a representation of the environment. The agent can then reason on this map and act efficiently towards its goal. How biological species map their environment is still an open area of research [1], [2]. In robotics, spatial representations have taken diverse forms, for instance metric maps [3], [4], [5] or topological maps [6], [7]. Most of these variants have lately been presented in neural counterparts — metric neural maps [8], [9], [10], [11] or neural topological maps [12], [13], [14] learned from RL or with supervision.

In this work, we explore the question whether the emergence of mapping and spatial reasoning capabilities can be favored by the use of spatial auxiliary tasks that are related to a downstream objective. We target the problem of *Multi-Object Navigation*, where an agent must reach a sequence of specified objects in a particular order within a previously unknown environment. Such a task is interesting because it requires an agent to recall the position of previously encountered objects it will have to reach later in the sequence.

We take inspiration from behavioral studies of human spatial navigation [15]. Experiments with human subjects

<sup>1</sup>Pierre Marza and Christian Wolf are with LIRIS, UMR CNRS 5205, Université de Lyon, INSA Lyon, Villeurbanne, France. pierre.marza@insa-lyon.fr, christian.wolf@insa-lyon.fr

<sup>2</sup>Laetitia Matignon is with LIRIS, UMR CNRS 5205, Université de Lyon, Univ. Lyon 1, Villeurbanne, France. laetitia.matignon@univ-lyon1.fr

<sup>3</sup>Olivier Simonin is with CITI Lab, Université de Lyon, INSA Lyon, INRIA Chroma team, Villeurbanne, France. olivier.simonin@insa-lyon.fr

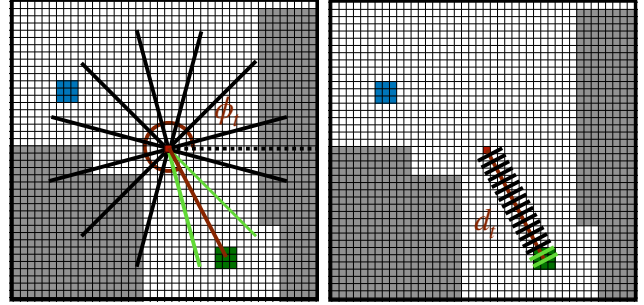


Fig. 1. In the context of Deep-RL for Multi-Object Navigation, two auxiliary tasks predict the direction (*left*) and the distance (*right*) to the next object to retrieve if it has been observed during the episode. The **green object** is the current target. Both, the angle  $\phi_t$  and the distance  $d_t$  between the center of the map (i.e. the agent) and the target at time  $t$  are discretized and associated with a class label. A third sub-task is to predict if the current target has already been within the agent’s field of view during the episode.

aim at evaluating the spatial knowledge they acquire when navigating a given environment. In [15], two important measures are referred as the *sense of direction* and *judgement of relative distance*. Regarding knowledge of direction, a well-known task is *scene- and orientation- dependent pointing* (SOP), where participants must point to a specified location that is not currently within their field of view. Being able to assess its relative position compared to other objects in the world is critical to navigate properly, and disorientation is considered a main issue. In addition to direction, evaluating the distance to landmarks is also of high importance.

We conjecture, that an agent able to estimate the location of target objects relative to its current pose will implicitly extract more useful representations of the environment and navigate more efficiently. A fundamental skill for such an agent is thus to remember previously encountered objects. Our auxiliary supervision targets exactly this ability. Classical methods based on RL rely on the capacity of the learning algorithm to extract mapping strategies from reward alone. While this has been shown to be possible in principle [9], we will show that the emergence of a spatial mapping strategy is significantly boosted through auxiliary tasks, which require the agent to continuously reason on the presence of targets w.r.t. to its viewpoint — see Figure 1.

We introduce three auxiliary tasks, namely estimating if a target object has already been observed since the beginning of the episode, and if it is the case, the relative direction and the Euclidean distance to this object. If an object is visible in the current observation, it will be helpful for training the agent to recognize it (discover its existence and relevance

to the task) and estimate its relative position, leading to an update of a latent spatially organized representation when the target was seen in the past.

We propose the following contributions: (i) we show that the auxiliary tasks improve the performance of previous baselines by a large margin, which even allows to reach the performance of (incomparable) agents using ground-truth oracle maps as input; (ii) we show the consistency of the gains over different agents with multiple inductive biases, reaching from simple recurrent models to agents structured with projective geometry. This raises the question whether spatial inductive biases are required or whether spatial organization can be learned; (iii) the proposed method reaches SOTA performance on the *Multi-ON* task, and corresponds to the winning entry of the *CVPR 2021 Multi-ON challenge*.

## II. RELATED WORK

**Visual navigation** — has thus been extensively studied in robotics [16], [17]. An agent is placed in an unknown environment and must solve a specified task based on visual input, where [16] distinguish map-based and map-less navigation. Recently, many navigation problems have been posed as goal-reaching tasks [18]. The nature of the goal, its regularities in the environment and how it is communicated to the agent have a significant impact on required reasoning capacities of the agent [19]. In *PointGoal* [18], an agent must reach a location specified as relative coordinates, while *ObjectGoal* [18] requires the agent to find an object of a particular semantic category. Recent literature [19], [20] introduced new navigation tasks with two important characteristics, (i) their sequential nature, i.e. an episode is composed of a sequence of goals to reach, and (ii) the use of external objects as target objectives.

*Multi-Object Navigation (MultiON)* [20] is a task requiring to sequentially retrieve objects, but unlike the *Ordered K-item* task [19], the order is not fixed between episodes. A sequential task is interesting as it requires the agent to remember and to map potential objects it might have seen while exploring the environment, as reasoning on them might be required in a later stage. Moreover, using external objects as goals prevents the agent from leveraging knowledge about the environment layouts, thus focusing solely on memory. Exploration is another targeted capacity as objects are placed randomly within environments. For these reasons, our work thus focuses on the new challenging *Multi-ON* task [20].

**Learning-free navigation** — A recurrent pattern in methods tackling visual navigation [16], [17] is modularity, with different computational entities solving a particular sub-part of the problem. A module might map the environment, another one localize the agent within this map, a third one performing planning. Low-level control is also often addressed by a specialized sub-module. Known examples are based on Simultaneous Localization and Mapping (SLAM) [4], [5].

**Learning-based navigation** — The task of navigation can be framed as a learning problem, leveraging the abilities of deep networks to extract regularities from a large amount of training data. Formalisms range from Deep Reinforcement

Learning (DRL) [21], [22], [23] to (supervised) Imitation Learning [24], [25], [26]. Such agents can be reactive [27], [23], but recent work tends to augment agents with memory, which is a key component, in particular in partially-observable environments [28], [29]. It can take the form of recurrent units [30], [31], or become a dedicated part of the system as in [32]. In the context of navigation, memory can fulfill multiple roles: holding a latent map-like representation of the spatial properties of the environment, as well as general high-level information related to the task (“*did I already see this object?*”). Common representations are metric [8], [9], [10], [11], or topological [12], [13], [14]. Other work reduces inductive biases by using Transformers [33] as a memory mechanism on episodic data [34], [35].

In contrast to end-to-end training, other approaches decompose the agent into sub-modules [36], [14] trained simultaneously with supervised learning [14] or a combination of supervised, reinforcement and imitation learning [36]. Somewhat related to our work, in [14], a dedicated semantic score prediction module is proposed, which estimates the direction towards a goal and is explicitly used to decide which previously unexplored ghost node to visit next inside a topological memory. In contrast, in our work we propose to predict spatial metrics such as relative direction as an auxiliary objective to shape the learnt representations, instead of explicitly using those predictions at inference time.

**Learning vs. learning-free** — The differences in navigation performance between SLAM-based and learning-based agents have been studied before [37], [38], [39]. Even though trained agents begin to perform better than classical methods in recent studies [39], arguments regarding efficiency of SLAM-based methods still hold [37], [38]. Frequently hybrid methods are suggested [36], [14]. In contrast, we explore the question, whether mapping strategies can emerge naturally in end-to-end training through additional pretext tasks.

**Auxiliary tasks** — can be combined with any downstream objective to guide a learning model to extract more useful representations as proposed in [21], [22] to improve, both, data efficiency and overall performance. [21] predict loop closure and reconstruct depth observations; Lample et al. [40] also augment the DRQN model [28] with predictions of game features in first-person shooter games. A potential drawback is the need for privileged information, which, however, is readily available in simulated environments [41], [42]. This is also the case in our work, where we access information during training on explored areas, positions of objects and of the agent, which, of course, is also used for reward generation in classical RL methods.

In [22], unsupervised objectives are introduced, such as pixel or action features and reward prediction. [43] introduce self-supervised auxiliary tasks to speed up the training on *PointGoal*. They augment the base agent from [44] with an inverse dynamics estimator as in [45], a temporal distance predictor, and an action-conditional contrastive module, which must differentiate between positives, i.e. real observations that occur after the given sequence, and negatives, i.e. observations sampled from other timesteps. [46]

introduce auxiliary tasks for *ObjectGoal*, building on top of [43] and introduce the action distribution prediction and generalized inverse dynamics tasks and coverage prediction.

Our work belongs to the group of supervised auxiliary tasks, with an application to 3D complex and photo-realistic environments, which was not the case of concurrent methods. We also specifically target the learning of mapping and spatial reasoning through additional supervision, which has not been the scope of previous approaches.

### III. LEARNING TO MAP

We target the *Multi-ON* task [20], where an agent is required to reach a sequence of target objects in a certain order, and which was used for a recent challenge organized in the context of the CVPR 2021 Embodied AI Workshop. Compared to much easier tasks like *PointGoal* or (Single) *Object Navigation*, *Multi-ON* requires more difficult reasoning capacities, in particular mapping the position of an object once it has been seen. The following capacities are necessary to ensure optimal performance: (i) mapping the object, i.e. storing it in a suitable latent memory representation; (ii) retrieving this location on request and using it for navigation and planning. This also requires to decide when to retrieve this information, i.e. solving a correspondence problem between sub-goals and memory representation.

The agent deals with sequences of objects that are randomly placed in the environment. At each time step, it only knows about the next object to find, which is updated when reached. The episode lasts until either the agent has found all objects in the correct order or the time limit is reached.

**Inductive agent biases** — Our contribution is independent of the actual inductive biases used for agents. We therefore explored several baselines with different architectures, as selected in [20]. The considered agents share a common base shown in Figure 2, which extracts information from the current RGB-D observation, and computes embeddings of the target object class and the previous action. Variants also keep a global map that is first transformed into an egocentric representation centered around the agent’s position (explained further below). The vector representations are concatenated and fed to a GRU [31] unit that integrates temporal information, and whose output serves as input to an actor and a critic heads. These two modules respectively predict a distribution  $\pi_\theta(a_t | s_t)$  over actions  $a_t$  conditioned on the current state  $s_t$  and the state-value function  $V^{\pi_\theta}(s_t) = \mathbb{E}_{a_t' \sim \pi_\theta} \left[ \sum_{t'=t}^T \gamma^{t'} R_{t'} | S_t = s_t \right]$ , i.e. expected cumulative reward starting in  $s_t$  and following policy  $\pi_\theta$ . The Actor-Critic algorithm is a baseline RL approach [47].

We consider different variants which have been explored in [20], but which have been introduced in prior work (numbers ①②③④ correspond to choices in Figure 2):

**NoMap** ① — is a recurrent GRU baseline without any spatial inductive bias.

**ProjNeuralMap** ①② [10], [9] — is a neural network structured with spatial information and projective geometry.

More specifically, ProjNeuralMap maintains a global allocentric map of the environment  $M_t \in \mathbb{R}^{H \times W \times n}$  composed

of  $n$ -channel vector representations at each position within the full  $H \times W$  environment. Similar to Bayesian occupancy grids (BOG), which have been used in mobile robotics for many years [48],[49], the map is updated in a two step process: (1) resampling taking into account estimated agent motion, and (2) integration of the current observation.

Writing to the map — Given the current RGB observation  $o_t \in \mathbb{R}^{h \times w \times 3}$ , a Convolutional Neural Network (CNN) extracts an  $n$ -channel feature map  $o'_t$ , which is then projected onto the 2D ground plane following the procedure in MapNet [10] to obtain an egocentric map of the agent’s spatial neighbourhood  $m_t \in \mathbb{R}^{h' \times w' \times n}$ . The ground projection module assigns a discrete location on the ground plane to each element within  $o'_t$  conditioned on the input depth map  $d_t \in \mathbb{R}^{h \times w}$  and known camera intrinsics. Registration of the observation  $m_t$  to the global map is based on the assumption that the agent has access to odometry, as in [20]. The update to  $M_t$  is performed through an element-wise max-pooling between  $m_t$  and  $M_{t-1}$ .

Reading the map — The controller reads the global map by first cropping around the agent and orienting it towards its current heading to form an egocentric map of its neighbourhood at time  $t$ , which is then fed to a CNN producing a context vector. The latter is then concatenated to the rest of the input, i.e. representations of the current observation, target object and previous action, producing the input to the recurrent memory (GRU) unit. The full model is trained end-to-end with Reinforcement Learning (RL), including networks involved in map writing and reading operations.

**OracleMap** ①③ — has access to a ground-truth grid map of the environment with 16 channels dedicated to occupancy information and 16 others to the presence of objects and their classes. The map is cropped and centered around the agent to produce an egocentric map as input to the model.

**OracleEgoMap** ①③④ — gets the same egocentric map as OracleMap with only object channels, and revealed in regions that have already been within its field of view during the episode. This variant corresponds to an agent capable of perfect mapping — no information gets lost, but only observed information is used.

#### A. Learning to map objects with auxiliary tasks

We introduce auxiliary tasks, additional to the classical RL objectives, and formulated as classification problems, which require the agent to predict information on object appearances, which were in its observation history in the current episode. To this end, the base model is augmented with three classification heads (Figure 2) taking as input the contextual representation produced by the GRU unit:

**Direction** — the agent predicts the relative direction of the target object, only if it has been within its field of view in the observation history of the episode (Figure 1 left). The ground-truth direction towards the goal is computed as,

$$\phi_t = \angle(\mathbf{o}_t, \mathbf{e}) = -\text{atan2}(\mathbf{o}_{t,x} - \mathbf{e}_x, \mathbf{o}_{t,y} - \mathbf{e}_y) \quad (1)$$

where  $\mathbf{e} = [\mathbf{e}_x \ \mathbf{e}_y]$  (“ego”) are the coordinates of the agent on the grid and  $\mathbf{o} = [\mathbf{o}_{t,x} \ \mathbf{o}_{t,y}]$  are the coordinates of the center

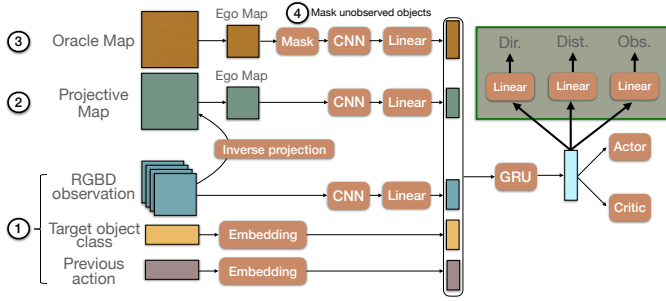


Fig. 2. To study the impact of our auxiliary losses on different agents [20], we explore several input and inductive biases. All variants share basic observations ① (RGB-D image, target class, previous action). Variants also use a map ② produced with inverse projective mapping. Oracle variants receive ground truth maps ③, where in one further variant unseen objects are removed ④. These architectures have been augmented with classification heads implementing the proposed auxiliary tasks (green rectangle).

of the target object at time  $t$ . As the ground-truth grid is egocentric, the position of the agent is fixed, i.e. at the center of the grid, while the target object gets different coordinates with time. The angles are kept in the interval  $[0, 2\pi]$  and then discretized into  $K$  bins, giving the angle class. The ground-truth one-hot vector is denoted  $\phi_t^*$ . At time instant  $t$ , the probability distribution over classes  $\hat{\phi}_t$  is predicted from the GRU hidden state  $\mathbf{h}_t$  through an MLP as  $p(\hat{\phi}_t) = f_\phi(\mathbf{h}_t; \theta_\phi)$  with parameters  $\theta_\phi$ .

**Distance** — The second task requires the prediction of the Euclidean distance in the egocentric map between the center box, i.e. position of the agent, and the mean of the grid boxes containing the target object (Figure 1 right) that was observed during the episode,

$$d_t = \|\mathbf{o}_t - \mathbf{e}\|_2. \quad (2)$$

Again, distances are discretized into  $L$  bins, with  $d_t^*$  as ground-truth one-hot vector, and at time instant  $t$ , the probability distribution over classes  $\hat{d}_t$  is predicted from the hidden state  $\mathbf{h}_t$  through an MLP as  $p(\hat{d}_t) = f_d(\mathbf{h}_t; \theta_d)$  with parameters  $\theta_d$ .

**Observed target** — This third loss favors learning whether the agent has previously encountered certain objects. The model is required to predict the binary value  $obs_t$ , defined as 1 if the target object at time  $t$  has been within the agent’s field of view at least once in the episode, and 0 otherwise. The model predicts the probability distribution over classes  $\hat{obs}_t$  given the hidden GRU state  $\mathbf{h}_t$  through an MLP as  $p(\hat{obs}_t) = f_{obs}(\mathbf{h}_t; \theta_{obs})$  with parameters  $\theta_{obs}$ .

**Training** — Following [20], all agents are trained with PPO [50] and a reward composed of three terms,

$$R_t = \mathbb{1}_t^{\text{reached}} \cdot R_{\text{goal}} + R_{\text{closer}} + R_{\text{time-penalty}} \quad (3)$$

where  $\mathbb{1}_t^{\text{reached}}$  is the indicator function whose value is 1 if the *found* action was called at time  $t$  while being close enough to the target, and 0 otherwise.  $R_{\text{closer}}$  is a reward shaping term equal to the decrease in geodesic distance to the next goal compared to previous timestep. Finally,  $R_{\text{time-penalty}}$  is a negative slack reward to force the agent to take short paths.

PPO alternates between sampling and optimization phases. At sampling time  $k$ , a set  $\mathcal{U}_k$  of trajectories  $\tau$  with length  $T$  are collected using the latest policy, where  $T$  is smaller than the length of a full episode. The base PPO loss is then,

$$\mathcal{L}_{PPO} = \frac{1}{|\mathcal{U}_k| T} \sum_{\tau \in \mathcal{U}_k} \sum_{t=0}^{T-1} \left[ \min \left( r_t(\theta) \hat{A}_t, \mathcal{C}(r_t(\theta), \epsilon) \hat{A}_t \right) \right] \quad (4)$$

where  $\mathcal{C}(r_t(\theta), \epsilon) = \text{clip}(r_t(\theta), 1 - \epsilon, 1 + \epsilon)$ ,  $\hat{A}_t$  is an estimate of the advantage function  $A^{\pi_\theta}(s_t, a_t) = Q^{\pi_\theta}(s_t, a_t) - V^{\pi_\theta}(s_t)$  at time  $t$  with  $Q^{\pi_\theta}(s_t, a_t) = \mathbb{E}_{a_{t'} \sim \pi_\theta} \left[ \sum_{t'=t}^T \gamma^{t'} R_{t'} \mid S_t = s_t, A_t = a_t \right]$ , and  $r_t(\theta) = \frac{\pi_\theta(a_t | s_t)}{\pi_{\theta_{\text{old}}}(a_t | s_t)}$  is the probability ratio between the updated and old versions of the policy. We did not make the dependency of states and actions on  $\tau$  explicit in the notation.

Direction, distance and observed target predictions are supervised with cross-entropy losses from ground truth values  $\phi_t^*$ ,  $d_t^*$  and  $\mathbb{1}_t^{\text{obs}}$ , respectively, as

$$\mathcal{L}_\phi = \frac{1}{|\mathcal{U}_k| T} \sum_{\tau \in \mathcal{U}_k} \sum_{t=0}^{T-1} \left[ -\mathbb{1}_t^{\text{obs}} \sum_{c=1}^K \phi_{t,c}^* \log p(\hat{\phi}_{t,c}) \right] \quad (5)$$

$$\mathcal{L}_d = \frac{1}{|\mathcal{U}_k| T} \sum_{\tau \in \mathcal{U}_k} \sum_{t=0}^{T-1} \left[ -\mathbb{1}_t^{\text{obs}} \sum_{c=1}^L d_{t,c}^* \log p(\hat{d}_{t,c}) \right] \quad (6)$$

$$\mathcal{L}_{obs} = \frac{1}{|\mathcal{U}_k| T} \sum_{\tau \in \mathcal{U}_k} \sum_{t=0}^{T-1} -(\mathbb{1}_t^{\text{obs}} \log p(\hat{obs}_t) + (1 - \mathbb{1}_t^{\text{obs}}) \log(1 - p(\hat{obs}_t))) \quad (7)$$

where  $\mathbb{1}_t^{\text{obs}}$  is the binary indicator function specifying whether the current target object has already been seen in the current episode ( $\mathbb{1}_t^{\text{obs}}=1$ ), or not ( $\mathbb{1}_t^{\text{obs}}=0$ ).

The auxiliary losses  $\mathcal{L}_\phi$ ,  $\mathcal{L}_d$  and  $\mathcal{L}_{obs}$  are added as follows,

$$\mathcal{L}_{\text{tot}} = \mathcal{L}_{PPO} + \lambda_\phi \mathcal{L}_\phi + \lambda_d \mathcal{L}_d + \lambda_{obs} \mathcal{L}_{obs} \quad (8)$$

where  $\lambda_\phi$ ,  $\lambda_d$  and  $\lambda_{obs}$  weight the relative importance of auxiliary losses.

## IV. EXPERIMENTAL RESULTS

We focus on the 3-ON version of the Multi-ON task, where the agent deals with sequences of 3 objects. The time limit is fixed to 2500 environment steps, and there are 8 object classes. The agent receives a  $(256 \times 256 \times 4)$  RGB-D observation and the one-in-K encoded class of the current target object within the sequence. The discrete action space is composed of four actions: *move forward* 0.25m, *turn left* 30°, *turn right* 30°, and *found*, which signals that the agent considers the current target object to be reached. As the aim of the task is to focus on evaluating the importance of mapping, a perfect localization of the agent was assumed as in the protocol proposed in [20].

**Dataset and metrics** — we used the standard train/val/test split over scenes from the Matterport [51] dataset, ensuring no scene overlap between splits. There are 61 training scenes, 11 validation scenes, and 18 test scenes. The train split consists of 50.000 episodes per scene, while there are 12.500

TABLE I

IMPACT OF DIFFERENT AUXILIARY TASKS (VALIDATION PERFORMANCE). THE † COLUMN SPECIFIES COMPARABLE AGENTS.

Agent	Dir.	Dist.	Obs.	Success	Progress	SPL	PPL	†
OracleMap	–	–	–	50.9± 2.4	61.2± 2.0	40.7± 1.9	48.8± 1.4	–
OracleEgoMap	–	–	–	34.1± 4.1	48.8± 3.8	27.9± 2.5	39.6± 2.2	–
	–	–	–	27.2± 2.9	44.6± 2.2	19.5± 0.7	32.3± 0.3	✓
ProjNeuralMap	–	–	✓	30.3± 5.0	47.7± 3.5	23.5± 3.5	36.6± 2.0	✓
	–	✓	–	34.4± 5.8	51.5± 4.3	25.1± 4.1	37.3± 3.3	✓
	✓	–	–	45.9± 6.9	61.2± 5.1	32.8± 5.0	43.7± 3.8	✓
	✓	✓	–	51.3 ± 7.8	65.5 ± 5.8	35.9 ± 5.3	46.0 ± 4.0	✓
	✓	✓	✓	<b>55.5 ± 4.8</b>	<b>68.9 ± 3.2</b>	<b>38.0 ± 2.2</b>	<b>47.5 ± 0.9</b>	✓

TABLE II

CONSISTENCY OVER MULTIPLE MODELS (TEST SET). THE † COLUMN SPECIFIES COMPARABLE AGENTS.

Agent	Aux. Sup.	Success	Progress	SPL	PPL	†
OracleMap	–	41.9± 3.0	52.7± 3.7	32.9± 1.9	41.1± 2.4	–
OracleEgoMap	–	22.3± 4.5	37.1± 5.1	17.4± 3.0	28.7± 2.7	–
	✓	31.4± 7.5	43.4± 7.3	23.5± 4.8	32.4± 4.4	–
ProjNeuralMap	–	17.9± 1.6	34.5± 2.1	12.2± 0.6	23.9± 0.6	✓
	✓	<b>41.4 ± 4.1</b>	<b>56.2 ± 3.1</b>	<b>27.0 ± 2.0</b>	<b>37.1 ± 1.7</b>	✓
NoMap	–	8.3± 1.4	22.8± 1.5	6.4± 0.6	17.6± 0.5	✓
	✓	30.7± 2.7	47.5± 3.3	18.6± 0.8	29.1± 0.7	✓

episodes per scene in the val and test splits. Reported results on the val and test sets (Tables I and II) were computed on a subset of 1000 randomly sampled episodes. We consider standard metrics of the field as given in [20]:

- *Success*: percentage of successful episodes (all three objects reached in the right order in the time limit).
- *Progress*: percentage of objects successfully found in an episode.
- *SPL*: Success weighted by Path Length. This extends the original SPL metrics from [18] to the sequential multi-object case.
- *PPL*: Progress weighted By Path Length.

Note that for an object to be considered found, the agent must take the *found* action while being within 1.5m of the current goal. The episode ends immediately if the agent calls *found* in an incorrect location. For more details, we refer to [20].

**Implementation details** — training and evaluation hyperparameters, as well as architecture details have been taken from [20]. All reported quantitative results are obtained after 4 training runs (6 runs were computed for *ProjNeuralMap* with the three auxiliary losses for job scheduling reasons) for each model, during 70M steps (increased from 40M in [20]). Ground-truth direction and distance measures are respectively split into  $K = 12$  and  $L = 36$  classes. Indeed, angle bins span  $30^\circ$ , and distance bins span a unit distance on the egocentric map, that is  $50 \times 50$  (the maximum distance between center and a grid corner is thus 35). Training weights  $\lambda_\phi$ ,  $\lambda_d$  and  $\lambda_{obs}$  are all fixed to 0.25.

**Do the auxiliary tasks improve the downstream objective?** — in Table I, we study the impact of the different auxiliary tasks on the 3-ON benchmark when added to the training objective of *ProjNeuralMap*, and their complementarity. Direction prediction significantly improves performance,

TABLE III

CVPR 2021 MULTI-ON CHALLENGE LEADERBOARD. *Test Challenge* ARE THE OFFICIAL CHALLENGE RESULTS. *Test Standard* CONTAINS PRE- AND POST-CHALLENGE RESULTS. RANKING IS DONE WITH **PPL**. THE \* SYMBOL DENOTES CHALLENGE BASELINES.

Agent/Method	— Test Challenge —				— Test Standard —			
	Success	Progress	SPL	PPL	Success	Progress	SPL	PPL
Ours (Aux. losses)	<b>55</b>	<b>67</b>	<b>35</b>	<b>44</b>	57	70	36	45
Team 2	52	64	32	38	62	71	34	39
Team 3	41	57	26	36	43	57	27	36
ProjNeuralMap*	–	–	–	–	12	29	6	16
NoMap*	–	–	–	–	5	19	3	13

adding distance prediction further increases the downstream performance by a large margin, outperforming the performance of (incomparable!) *OracleEgoMap*. Both losses have thus a strong impact and are complementary, confirming the assumption that *sense of direction* and *judgement of relative distance* are two key skills for spatially navigating agents. The third loss about observed target objects brings a supplementary non-negligible boost in performance, showcasing the effectiveness of explicitly learning to remember, and its complementarity with distance and direction prediction.

Table II presents results on the test set, confirming the significant impact on each of the considered metrics. *ProjNeuralMap* with auxiliary losses matches the performance of (incomparable!) *OracleMap* on Progress and Success, again outperforming *OracleEgoMap* when considering all metrics. *OracleMap* has higher PPL and SPL, but has also access to very strong privileged information.

**Can an unstructured recurrent agent learn to map?** — we explore whether an agent without spatial inductive bias can be trained to learn a mapping strategy, to encode spatial properties of the environment into its unstructured hidden representation. As shown in Table II, *NoMap* indeed strongly benefits from the auxiliary supervision (Success for instance jumping from 8.3% to 30.7%). Improvement is significant, outperforming *ProjNeuralMap* trained with vanilla RL, and closing the gap with *OracleEgoMap*. The quality of extra supervision can thus help to guide the learnt representation, mitigating the need for incorporating inductive biases into neural networks. When both are trained with our auxiliary losses, *ProjNeuralMap* still outperforms *NoMap*, indicating that spatial inductive bias still provides an edge.

**Comparison with the state-of-the-art** — our method corresponds to the winning entry of the *CVPR 2021 Multi-On Challenge* organized with the *Embodied AI Workshop*, shown in Table III. Test-standard is composed of 500 episodes and Test-challenge of 1000 episodes. In the context of the Challenge, the *ProjNeuralMap* agent was trained for 80M steps with the auxiliary objectives, and then finetuned for 20M more steps with only the vanilla RL objective. The official challenge ranking is done with **PPL**, which evaluates correct mapping (quicker and more direct finding of objects), while mapping does not necessarily have an impact on success rate, which can be obtained by pure exploration.

**Visualization** — Figure 3 illustrates an example trajectory

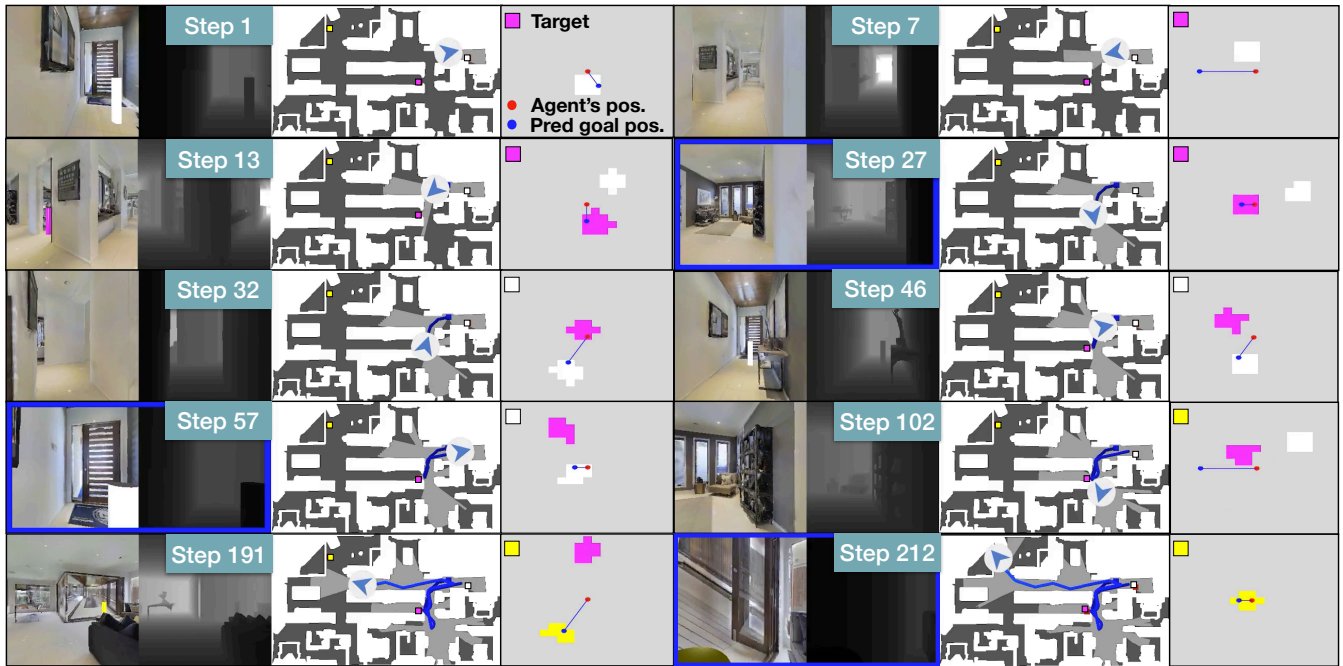


Fig. 3. Example agent trajectory (sample from competition Mini-val set). The agent properly explores the environment to find the pink object. It then successfully backtracks to reach the white cylinder, and finally goes to the yellow one after another exploration phase (see text for a detailed description). In columns 3 and 6, the relative direction and distance predictions are combined into a visualised blue point on top of the oracle egocentric map (Ground-truth object positions). The red point corresponds to the position of the agent. Note that these predictions are not used by the agent at inference time, and are only shown for visualisation purposes. The top down view and oracle egocentric map are also provided for visualisation only.

from the agent trained with the auxiliary supervision in the context of the *CVPR 2021 Multi-On Challenge*. The agent starts the episode (Step 1) seeing the white object, which is not the first target to reach. It thus starts exploring the environment (Step 7), until seeing the pink target object (Step 13). Its prediction of the goal distance immediately improves, showing it is able to recognize the object within the RGB-D input. The agent then reaches the target (Step 27). The new target is now the white object (that was seen in Step 1). While it is still not within its current field of view, the agent can localize it quite precisely (Step 32), and go towards the goal (Step 46) to call the *found* action (Step 57). The agent must then explore again to find the last object (Step 105). When the yellow cylinder is seen, the agent can estimate its relative position (Step 191) before reaching it (Step 212) and ending the episode.

**Information about observed targets, their relative distance and direction** — Is such knowledge extracted by *ProjNeuralMap* without auxiliary supervision? We perform a probing experiment by training three linear classifiers to predict this information from the contextual representation from the GRU unit, both for *ProjNeuralMap* agent initially trained with and without auxiliary losses. We generate rollout trajectories on 1000 training and validation episodes. It is important to note that, as both agents behave differently, linear probes are not trained and evaluated on the same data. Fig. 4 shows that linear probes trained on representations from our method perform better, and more consistently, suggesting the presence of more related spatial information.

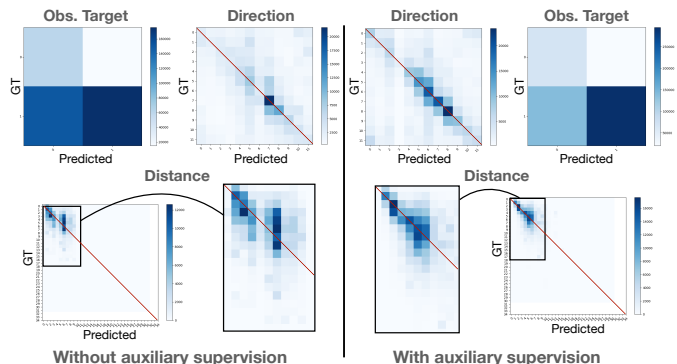


Fig. 4. Confusion matrices (validation set) of linear probes trained on representations from both *ProjNeuralMap* initially optimized with and without auxiliary supervision. Red lines indicate matrix diagonals.

## V. CONCLUSION

In this work, we propose to guide the learning of mapping and spatial reasoning capabilities by augmenting vanilla RL training objectives with auxiliary tasks. We show that learning to predict the relative direction and distance of already seen target objects, as well as to keep track of those observed objects, improves significantly the performance on various metrics and that these gains are consistent over agents with or without spatial inductive bias. We reach SOTA performance on the Multi-ON benchmark. Future work will investigate additional structure, for instance predicting multiple objects.

## REFERENCES

- [1] M. Peer, I. K. Brunec, N. S. Newcombe, and R. A. Epstein, "Structuring knowledge with cognitive maps and cognitive graphs," *Trends in Cognitive Sciences*, 2020.
- [2] W. H. Warren, D. B. Rothman, B. H. Schnapp, and J. D. Ericson, "Wormholes in virtual space: From cognitive maps to cognitive graphs," *Cognition*, 2017.
- [3] A. Elfes, "Using occupancy grids for mobile robot perception and navigation," *Computer*, 1989.
- [4] G. Bresson, Z. Alsayed, L. Yu, and S. Glaser, "Simultaneous localization and mapping: A survey of current trends in autonomous driving," *IEEE Transactions on Intelligent Vehicles*, 2017.
- [5] H. Durrant-Whyte and T. Bailey, "Simultaneous localization and mapping: part i," *IEEE robotics & automation magazine*, 2006.
- [6] H. Shatkay and L. P. Kaelbling, "Learning topological maps with weak local odometric information," in *IJCAI*, 1997.
- [7] S. Thrun, "Learning metric-topological maps for indoor mobile robot navigation," *Artificial Intelligence*, 1998.
- [8] E. Parisotto and R. Salakhutdinov, "Neural map: Structured memory for deep reinforcement learning," in *International Conference on Learning Representations*, 2018.
- [9] E. Beeching, J. Dibangoye, O. Simonin, and C. Wolf, "Egomap: Projective mapping and structured egocentric memory for deep RL," in *ECML-PKDD*, 2020.
- [10] J. F. Henriques and A. Vedaldi, "Mapnet: An allocentric spatial memory for mapping environments," in *IEEE/CVF Conference on Computer Vision and Pattern Recognition*, 2018.
- [11] S. Gupta, J. Davidson, S. Levine, R. Sukthankar, and J. Malik, "Cognitive mapping and planning for visual navigation," in *IEEE/CVF Conference on Computer Vision and Pattern Recognition*, 2017, pp. 2616–2625.
- [12] E. Beeching, J. Dibangoye, O. Simonin, and C. Wolf, "Learning to plan with uncertain topological maps," in *European Conference on Computer Vision 2020*, 2020.
- [13] N. Savinov, A. Dosovitskiy, and V. Koltun, "Semi-parametric topological memory for navigation," in *International Conference on Learning Representations*, 2018.
- [14] D. S. Chaplot, R. Salakhutdinov, A. Gupta, and S. Gupta, "Neural topological slam for visual navigation," in *IEEE/CVF Conference on Computer Vision and Pattern Recognition*, 2020.
- [15] A. D. Ekstrom, H. J. Spiers, V. D. Bohbot, and R. S. Rosenbaum, *Human spatial navigation*. Princeton University Press, 2018.
- [16] F. Bonin-Font, A. Ortiz, and G. Oliver, "Visual navigation for mobile robots: A survey," *Journal of intelligent and robotic systems*, 2008.
- [17] S. Thrun, W. Burgard, D. Fox *et al.*, "Probabilistic robotics, vol. 1," 2005.
- [18] P. Anderson, A. X. Chang, D. S. Chaplot, A. Dosovitskiy, S. Gupta, V. Koltun, J. Kosecka, J. Malik, R. Mottaghi, M. Savva, and A. R. Zamir, "On evaluation of embodied navigation agents," *arXiv preprint*, 2018.
- [19] E. Beeching, J. Dibangoye, O. Simonin, and C. Wolf, "Deep reinforcement learning on a budget: 3d control and reasoning without a supercomputer," in *International Conference on Pattern Recognition*, 2020.
- [20] S. Wani, S. Patel, U. Jain, A. X. Chang, and M. Savva, "Multion: Benchmarking semantic map memory using multi-object navigation," in *Advances in Neural Information Processing Systems*, 2020.
- [21] P. Mirowski, R. Pascanu, F. Viola, H. Soyer, A. Ballard, A. Banino, M. Denil, R. Goroshin, L. Sifre, K. Kavukcuoglu, D. Kumaran, and R. Hadsell, "Learning to navigate in complex environments," in *International Conference on Learning Representations*, 2017.
- [22] M. Jaderberg, V. Mnih, W. M. Czarnecki, T. Schaul, J. Z. Leibo, D. Silver, and K. Kavukcuoglu, "Reinforcement learning with unsupervised auxiliary tasks," in *International Conference on Learning Representations*, 2017.
- [23] Y. Zhu, R. Mottaghi, E. Kolve, J. J. Lim, A. Gupta, L. Fei-Fei, and A. Farhadi, "Target-driven visual navigation in indoor scenes using deep reinforcement learning," in *International Conference on Robotics and Automation*, 2017.
- [24] Y. Ding, C. Florensa, P. Abbeel, and M. Phielipp, "Goal-conditioned imitation learning," in *Advances in Neural Information Processing Systems*, 2019.
- [25] D. Watkins-Valls, J. Xu, N. Waytowich, and P. Allen, "Learning your way without map or compass: Panoramic target driven visual navigation," *arXiv preprint*, 2019.
- [26] Q. Wu, X. Gong, K. Xu, D. Manocha, J. Dong, and J. Wang, "Towards target-driven visual navigation in indoor scenes via generative imitation learning," *arXiv preprint*, 2020.
- [27] A. Dosovitskiy and V. Koltun, "Learning to act by predicting the future," in *International Conference on Learning Representations*, 2017.
- [28] M. Hausknecht and P. Stone, "Deep recurrent q-learning for partially observable mdps," in *AAAI Conference on Artificial Intelligence*, 2015.
- [29] J. Oh, V. Chockalingam, Satinder, and H. Lee, "Control of memory, active perception, and action in minecraft," in *International Conference on Machine Learning*, 2016.
- [30] S. Hochreiter and J. Schmidhuber, "Long short-term memory," *Neural Comput.*, 1997.
- [31] K. Cho, B. van Merriënboer, C. Gulcehre, D. Bahdanau, F. Bougares, H. Schwenk, and Y. Bengio, "Learning phrase representations using RNN encoder–decoder for statistical machine translation," in *Conference on Empirical Methods in Natural Language Processing*, 2014.
- [32] A. Graves, G. Wayne, and I. Danihelka, "Neural turing machines," *arXiv preprint*, 2014.
- [33] A. Vaswani, N. Shazeer, N. Parmar, J. Uszkoreit, L. Jones, A. N. Gomez, Ł. Kaiser, and I. Polosukhin, "Attention is all you need," in *Advances in Neural Information Processing Systems*, 2017.
- [34] S. Ritter, R. Faulkner, L. Sartran, A. Santoro, M. Botvinick, and D. Raposo, "Rapid task-solving in novel environments," in *International Conference on Learning Representations*, 2021.
- [35] K. Fang, A. Toshev, L. Fei-Fei, and S. Savarese, "Scene memory transformer for embodied agents in long-horizon tasks," in *IEEE/CVF Conference on Computer Vision and Pattern Recognition*, 2019.
- [36] D. S. Chaplot, D. Gandhi, S. Gupta, A. Gupta, and R. Salakhutdinov, "Learning to explore using active neural slam," in *International Conference on Learning Representations*, 2020.
- [37] D. Mishkin, A. Dosovitskiy, and V. Koltun, "Benchmarking classic and learned navigation in complex 3d environments," *arXiv preprint*, 2019.
- [38] N. Kojima and J. Deng, "To learn or not to learn: Analyzing the role of learning for navigation in virtual environments," *arXiv preprint*, 2019.
- [39] M. Savva, A. Kadian, O. Maksymets, Y. Zhao, E. Wijmans, B. Jain, J. Straub, J. Liu, V. Koltun, J. Malik, D. Parikh, and D. Batra, "Habitat: A platform for embodied ai research," in *IEEE/CVF International Conference on Computer Vision*, 2019.
- [40] G. Lample and D. S. Chaplot, "Playing fps games with deep reinforcement learning," in *AAAI Conference on Artificial Intelligence*, vol. 31, no. 1, 2017.
- [41] M. Kempka, M. Wydmuch, G. Runc, J. Toczek, and W. Jaśkowski, "Vizdoom: A doom-based ai research platform for visual reinforcement learning," in *IEEE Conference on Computational Intelligence and Games*, 2016.
- [42] C. Beattie, J. Z. Leibo, D. Teplyaev, T. Ward, M. Wainwright, H. Küttler, A. Lefrancq, S. Green, V. Valdés, A. Sadik *et al.*, "Deepmind lab," *arXiv preprint*, 2016.
- [43] J. Ye, D. Batra, E. Wijmans, and A. Das, "Auxiliary tasks speed up learning pointgoal navigation," *arXiv preprint*, 2020.
- [44] E. Wijmans, A. Kadian, A. Morcos, S. Lee, I. Essa, D. Parikh, M. Savva, and D. Batra, "Dd-ppo: Learning near-perfect pointgoal navigators from 2.5 billion frames," in *International Conference on Learning Representations*, 2019.
- [45] D. Pathak, P. Agrawal, A. A. Efros, and T. Darrell, "Curiosity-driven exploration by self-supervised prediction," in *International Conference on Machine Learning*, 2017.
- [46] J. Ye, D. Batra, A. Das, and E. Wijmans, "Auxiliary tasks and exploration enable objectnav," *arXiv preprint*, 2021.
- [47] R. S. Sutton and A. G. Barto, *Reinforcement learning: An introduction*. MIT press, 2018.
- [48] H. Moravec, "Sensor fusion in certainty grids for mobile robots," *AI magazine*, vol. 9, no. 2, 1988.
- [49] L. Rummelhard, A. Nègre, and C. Laugier, "Conditional Monte Carlo Dense Occupancy Tracker," in *ITSC*, 2015.
- [50] J. Schulman, F. Wolski, P. Dhariwal, A. Radford, and O. Klimov, "Proximal policy optimization algorithms," *arXiv preprint*, 2017.
- [51] A. Chang, A. Dai, T. Funkhouser, M. Halber, M. Niebner, M. Savva, S. Song, A. Zeng, and Y. Zhang, "Matterport3d: Learning from rgb-d data in indoor environments," in *IEEE International Conference on 3D Vision*, 2018.